



Electronic Structures and Optical Properties of TiO₂ DSSC Investigated by Computer Simulation

¹T. Ranganayaki, ²M. Venkatachalam, ²T. Vasuki, ²S. Shankar

¹Department of Computer Science, Erode Arts and Science College, Erode-9, Tamil Nadu.

²Thin Film Center, Research Department of Electronics, Erode Arts and Science College, Erode-9, Tamil Nadu.

Abstract : Ruthenium pyridine-derivative complexes are used in dye-sensitized solar cell TiO₂ [DSSC] as a light to current conversion sensitizer. In order to improve the efficiency of the TiO₂ DSSC the noble metal ruthenium and some compounds present in the electrolyte (consists of 0.6M of 1-butyl-3-methylimidazolium iodide (BMII), 0.03M iodine, 0.06 M Lithium iodide 0.5 M 4-tetra-butylpyridine, 0.1 M guanidinium thiocyanate). The geometries, electronic structures and optical absorption spectra of these compounds have been studied by using density functional theory (DFT) calculation at the B3LYP/LANL2DZ, B3LYP/GEN level of theory. All the geometric parameters are close to the experimental values. HOMOs are mainly on the electrolyte groups mixed with fewer characters of the metal atom, the LUMOs are mainly on the two pyridine ligands. This means that the electron transition is attributed to the absorption layer. The maximum absorptions of complexes are found to be at 400 nm for the compounds. This means that those compounds may be as a suitable sensitizer for solar energy conversion applications. The performance of the TiO₂ DSSC solar cells have been confirmed with computer simulation using VASP.

Keywords : DSSC, DFT, GEN, HOMO, LUMO, VASP.

Introduction

Crystal structure prediction starting from the chemical composition alone has been one of the long-standing challenges in theoretical solid state physics, chemistry, and materials science [1, 2]. Progress in this area has become a pressing issue in the age of computational materials discovery and design. In the past two decades several computational methods have been proposed to tackle this problem. These methods include simulated annealing [3–5], genetic algorithm (GA) [6–13], basin (or minima) hopping [14, 15], particle swarm optimization [16, 17], and ab initio random structure search [18]. While there has been steady progress in predicting the crystal structures of elementary crystals, oxides, and binary alloys [8–13, 16–18], exploration of complex binary, ternary, and quaternary systems has required more advanced algorithms for configuration space exploration and faster but reliable methods for energy evaluation. While first-principles density functional theory (DFT) calculations offer accurate total energies, the computational cost imposes a bottleneck to the structure identification of complex materials with unit cells containing 102 atoms and/or with variable stoichiometries. By contrast, calculations based on classical potentials are fast and applicable to very large systems but are limited in accuracy. For various systems, reliable classical potentials are not even available. We present in this paper an adaptive-GA that combines the speed of classical potential searches and the accuracy of first-principles DFT calculations. It allows us to investigate crystal structures previously intractable by such methods with current computer capabilities. The left-hand side of the flowchart is the traditional GA loop. The GA is an optimization strategy inspired by the Darwinian evolutionary process and has been widely adopted for atomistic structure optimization in the last 18 years [6–13]. During the GA optimization process, inheritance, mutation, selection, and crossover operations [6–13] are included to produce new structures and select the most

fit survivors from generation to generation. The most time-consuming step in the traditional GA-loop is the local optimization of new offsprings by DFT calculations. For complex structures, GA search usually iterates over 200 generations to converge.

In the adaptive-GA scheme this most time-consuming step is performed using auxiliary classical potentials. In the adaptive-loop, single point DFT calculations are performed on a small set of candidate structures obtained in the GA-loop using the auxiliary classical potentials. Energies, forces, and stresses of these structures from first-principles DFT calculations are used to update the parameters of the auxiliary classical potentials by a force-matching method with a stochastic simulated annealing algorithm as implemented in the potfit code [19, 20]. Another cycle of GA search is performed using the newly adjusted potentials, followed by the re-adjustment of the potential parameters, and the process is then repeated—an adaptive-GA (AGA) iteration. All first-principles DFT calculations were performed using VASP [21- 26] packages, interfaced with the adaptive-GA scheme in a fully parallel manner.

Computational Details

5.3.1. Calculation Method

Calculations of the band gap, density of states, optical spectra and electronic properties of the crystals TiO₂ have been performed using the VASP code, a DFT plane wave pseudo-potential program within the framework of local density approximation (LDA) and generalized gradient approximation (GGA) Perdew-Wang 91 for the exchange correlation effects. However, GGA is definitely a more accurate tool when energy calculation is involved, and it is also a preferred way of describing system with weak bonding (molecular crystals). The ultra-soft model pseudo-potentials are used. This pseudo-potential require a quite low energy cut off and guarantee good transferability, that is the same potential correctly reproduces the valence electron scattering by the ion core in different chemical environments. Calculations are performed using the plane wave basis set with the kinetic energy cut off for plane wave 340 eV, which corresponds to the energy convergence criterion of self-consistency of 0.2×10^{-5} eV/atom. The optimization of crystal structure has been performed with the characteristic tolerances for total energy 0.2×10^{-4} eV /atom, and root mean square stress tensor 0.1GPa, before the calculations of band structure. Each energy state of the crystals is calculated at 23 k-points of Brillouin zone.

5.3.2. Structural Optimization

The crystal structure and locations of the particular atoms of the TiO₂ have been determined from X-ray diffraction data. The cutoff energy of 3.40 eV was assumed in the plane wave basis set. Optimization (relaxation) of the atomic positions and crystal cell parameters was performed before the main calculations of electronic characteristic: total electronic energy E , band energy dispersion, density of electronic states and dielectric functions.

5.3.3 Density of States and Partial Density of States

The density of states for a given band n , $N_n(E)$ is defined as $N_n(E) = \int \frac{dk}{4\pi^3} \delta(E - E_n(k))$ where $E_n(k)$ describes the dispersion of the given band and the integral is determined over the Brillouin zone. An alternative representation of the density of states is based on the fact that $N_n(E)dE$ is proportional to the number of allowed wave vectors in the n^{th} band in the energy range from E to $E+dE$. The total density of states $N(E)$, is obtained by summation over all bands. The integral of $N(E)$ from minus infinity to the Fermi level gives the total number of electrons in the unit cell. In a spin-polarized system one can introduce separate DOS for electrons with spin up and those with spin down. Their sum produces the total DOS and their difference is referred to as a spin density of states. The DOS is a useful mathematical concept allowing integration with respect to electron energy to be used instead of the integration over the Brillouin zone. In addition, the DOS is often used for quick visual analysis of the electronic structure. Characteristics such as the width of the valence band, the energy gap in insulators and the number and intensity of the main features are helpful in qualitatively interpreting experimental spectroscopic data. DOS analysis can help to understand the changes in electronic structure caused by, for example, external pressure. There exist a variety of numerical techniques for evaluating the DOS. The simplest one is based on the Gaussian smearing of the energy levels of each band, followed by a

histogram sampling. This method does not reproduce sharp features of the DOS, such as van-Hove singularities but it produces a satisfactory general shape of the DOS even with a small number of k-points used.

Partial density of states (PDOS) and local density of states (LDOS) represent useful semi-qualitative tools for analyzing electronic structure. LDOS shows which atoms in the system contribute electronic states to various parts of the energy spectrum. PDOS further qualifies these results by resolving these contributions according to the angular momentum of the states. It is often useful to know whether the main peaks in the DOS are of s, p, or d character. LDOS and PDOS analyses give a qualitative handle on the nature of electron hybridization in the system, on the region of the main features in optical spectra etc. PDOS calculations are based on Mulliken population analysis which allows us to calculate the contribution from each energy band to a given atomic orbital. Summation of these contributions over all bands produces weighted DOS. CASTEP allows us to select the type of weighting required. It is possible, for example, to generate LDOS by adding together all the contributions due to orbitals on a given atom. The calculation itself can be carried out using either Gaussian smearing or linear interpolation, similar to the total DOS calculation. In this case, the latter method includes the interpolation of the weights as well as the electronic energies.

Results and Discussion

ab initio Studies of Structural Properties

X ray diffraction results of the thin films reveals that they are Nanocrystalline nature with the prominent peak positions the dominant structure of TiO_2 identified. The positions of the Ti and O atoms are not defined experimentally and they are taken with different possible conditions, such that the results (XRD, band structure) are matched with the experimental values. Figure 1 shows the structure of TiO_2 Anatase. The structure of TiO_2 are found to be Anatase structure with the unit cell dimensions $a = 3.776 \text{ \AA}$ and $c = 9.486 \text{ \AA}$ with the number of formula units in the unit cell are 4 and 2 respectively. This TiO_2 structures are constructed using the VASP by fixing the atoms in a cube to form Anatase structure in cell. The constructed structures are optimized using the VASP module. The self consistent method of convergence of the structure is used to optimize the lattice parameters; the X-ray diffraction is simulated these XRD results are similar to that of the experimental XRD with the slight deviation of 0.015 % and 0.016 % for CIGS respectively. The XRD spectra of the unit cells of TiO_2 are simulated and peak positions are analyzed.

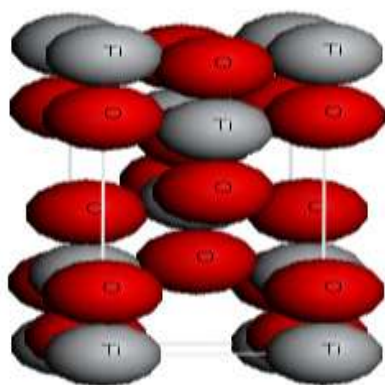


Figure 1 Structure of TiO_2 Anatase

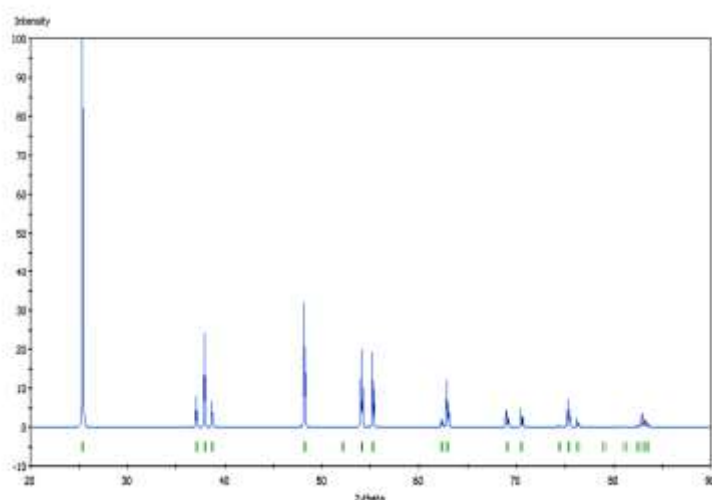


Figure 2 Simulated XRD pattern of TiO₂ structure

Table 1 Miller indices of TiO₂ structure

h	k	l	2 θ (Simulated)	Intensity (%)
1	0	1	25.773	100
1	1	2	39.310	12
2	0	0	48.459	36
2	1	1	56.028	25
2	1	3	63.25	16.4
2	1	5	76.3	5

Using Materials Studio Software in the CASTEP module, the pseudo atomic calculation was performed for Oxygen ($2s^2 2p^4$) and Converged in 26 iterations to a total energy of -428.636711 eV. Similarly the pseudo atomic calculation was performed for Titanium ($3s^2 3p^6 3d^2 4s^2$) and converged in 33 iterations to a total energy of -1594.961302 eV.

The results of the electronic minimization in the TiO₂ are i) total energy / atom convergence 10^{-6} eV, ii) eigen energy convergence tolerance 0.2308×10^{-6} eV, iii) convergence tolerance window 3 cycles, iv) maximum number of SCF cycles 100, v) number of fixed-spin iterations 10, vi) smearing scheme Gaussian smearing width 0.1eV, vii) Fermi energy convergence tolerance 0.2308×10^{-7} eV.

The TiO₂ anatase was geometrically optimized with the parameters i) total energy convergence tolerance 0.1×10^{-4} eV/atom, ii) max ionic force tolerance 0.3×10^{-1} eV/Å, iii) max ionic displacement tolerance 0.10×10^{-2} Å, iv) max stress component tolerance 0.5×10^{-1} GPa, v) convergence tolerance window 2 steps, vi) backup results every 5 steps.

The optimized anatase unit cell parameters of the TiO₂ are as follows

i) $a = 3.776$ Å, ii) $b = 3.776$ Å, iii) $c = 9.486$ Å, iv) cell volume = 135.25 (Å)³ and v) interfacial angles $\alpha = \beta = \gamma = 90^\circ$. The final self consistency energy of the structure is found to be from -9924.330021421 eV to -9924.330574135 eV with the enthalphy -9.92433057×10^3 eV.

From the self-consistent method of convergence results the lattice parameters are optimized and they are found to be very similar to the experimental results.

ab initio studies of electronic properties

The calculations of electronic characteristics; total electronic energy E , band energy dispersion $E(k)$, density of states of TiO₂ structures are simulated using the VASP code. For TiO₂ 72 electrons (36 up spins and

36 down spins) and 48 bands are as chosen as electronic parameters. The total energy per atom convergence, eigen-energy convergence tolerance, smearing width and Fermi energy convergence tolerance are taken as 0.2×10^{-5} eV, 0.4×10^{-6} eV, 0.1 eV and 0.4×10^{-7} eV respectively are taken as electronic minimization parameters.

Band structure of the crystal is calculated of 48 band of the Brillouin zone with band convergence tolerance of 0.1×10^{-4} eV and 4 k-points are considered for Brillouin zone sampling. From the above simulations it is found that the density of states of the structure is nearly same from the LDA and GGA. The band gap energy of TiO₂ are determined from the band structures (gamma point) and density of states results it is found that the values are nearly 2.42 eV which are smaller than the experimentally determined values. The percentages of deviation of the results are in the order of 20%.

Conclusion

The performance of the TiO₂ DSSC solar cells are have been confirmed with computer simulation using VASP. The structural optimization, density of states and partial density of states have been simulated using VASP. From the self-consistent method of convergence results the lattice parameters are optimized and they are found to be very similar to the experimental results.

References:

1. B. Oregan and M. Gratzel, *nature*, 353, (1991) 737.
2. D. Wei and G. Amaratunga, *Int. J. Electrochem. Sci.*, 2 (2007) 897.
3. M.H. Lai, M. W. Lee, G.J. Wang and m.F. Tai, *Int. J. Electrochem. Sci.*, 6 (2011) 2122.
4. A. Yella, H.W. Lee, H.N. Tsao, C.Y.Yi, a.K. Chandiran, M.K. Nazeeruddin, E.W.G. Diau, C.Y.Yeh, S.M.Zakeeruddin and M.Gratzel, *Science*, 334 (2011) 629.
5. E. Figgemeier and A. Hagfeldt, *Int. J. Photoenergy*, 6 (2004) 127.
6. M. I. Asghar, K. Miettunen, J. Halme, P. Vahermaa, M. Toivola, K. Aitola and P. Lund, *energ. Environ. Sci.*, 3 (2010) 418.
7. M. Gratzel, *Cr. Chim.*, 9 (2006) 578.
8. M. Toivola, J. Halme, L. Peltokorpi and P. Lund, *Int. J. Photoenergy*, (2009), DOI: 10.1155/2009/786429.
9. A. Hinsch, J. M. Kroon, R. Kern, I. Uhlendorf, J. Holzbock, A. Meyer and J. Ferber, *Prog. Photovoltaics*, 9 (2001) 425.
10. S. Y. Dai, J. Weng, Y. F. Sui, S. H. Chen, s.F. Xiao, Y. Huang, F.T.Kong, X. Pan, L. H. Hu, C.N.Zhang and K.J.Wang, *Inorg. Chim. Acta*, 361 (2008) 786.
11. Y. Takeda, N. Kato, K. Higuchi, A. Takeichi, T.Motohiro, S.Fukumoto, t. Sano and T. Toyoda, *sol. Energ. Mat. Sol. C.*, 93 (2009) 808.
12. H. Petterssoon and T. Gruszecki, *sol. Energ. Mat. Sol. C.*, 70 (2001) 203.
13. H. Matsui, K. Okada, T.Kitamura and N. Tanabe, *sol. Energ. Mat. Sol. C.*, 93 (2009) 1110.
14. P.M. Sommeling, M. Spath, H.J.P.Smit, N.J.Bakker and J.M.Kroon, *J.Photoch. Photobio. A*, 164 (2004) 137.
15. N. Kato, Y. Takeda, K. Higuchi, A. Takeichi, E. Sudo. H. Tanaka, T. Motohiro, T.Sano and T.Toyoda, *sol. Energ. Mat. Sol. C.*, 93 (2009) 893.
16. H. Greijer, J. Lindgren and A. Hagfeldt. *J. Phys. Chem. B*. 105 (2001) 6314.
17. S. . Ito, P.Chen, P.Comte, M.K.Nazeeruddin, P.Liska, P.Pechy and M. Gratzel, *Prog. Photovoltaics*, 15 (2007) 603.
18. A.D. Becke, *J Chem Phys*, 98 (1993) 5648.
19. C.T.Lee, W.T.Yang and R.G. Parr, *Phys. Rev. B*, 37 (1988) 785.
20. M.J.Frish, G.W.Truckes, H.B.Schlegel, G.E.Scuseria, M.a.Robb, J.R.Cheeseman, Et al. *Gaussian 03*, Revision E.01, gaussian Inc: Wallingford, CT 2004.
21. L.Q.Xiong, Q.Zhao, H.L.Chen, Y.B.Wu, Z.S.Dong, Z.G.Zhou and F.Y.Li, *Inorg, Chem.*, 49 (2010) 6402.
22. M. Ni, M.K.H.Leung and D.Y.C.Leung, *Can. J. Chem. Eng.*, 86 (2008) 35.
23. N. Koide, A. Islam, Y. Chiba and L.Y.Han, *J.Photoch Photobio. A*, 182 (2006) 296.
24. R.H. Bari, Selectivity of organic vapour for nanostructured CdO thin films prepared by sol-gel dip coating technique, *International Journal of Chemical Concepts*, 2015, 1 (3), 136-148.

25. R. H. Bari, S. B. Patil Improved NO₂ sensing performance of nanostructured Zn doped SnO₂ thin films, International Journal of Chemical Concepts, 2015, 1 (2), 86-96.
26. R. H. Bari S. B. Patil Ethanol sensing performance of nanostructured Zn doped CdSnO₃ thin films International Journal of Chemical Concepts, 2016, 2 (1), 01-11.
